Influences of radiation from terrestrial power sources on the ionosphere above China based on satellite observation

Chong Zhang and Qishuang Ma

School of automation science and electrical engineering,
Beihang University, Beijing, 100191, China

308639228@qq.com

Abstract. The environmental effect on the ionosphere caused by man-made power line emission (PLE) and power line harmonic radiation (PLHR) has become an increasing concern. Based on the observed data of 6.5 operating years of DEMETER satellite, by scanning the electric field power density time-frequency spectrograms, 133 PLHR events with central frequencies from 500 Hz to 4.5 kHz are detected in the near-Earth space above China. The fundamental frequency related well to the frequency of corresponding ground power system. Among the 133 events, 129 events have PLE events at the base power system frequency (50 Hz in China). The duration time of every PLE event covers that of the corresponding PLHR event totally. As the same with PLHR, PLE is also propagating in whistler mode in the ionosphere. In two events that are detected in the conjugate region of Australian NWC VLF transmitter, radiations with line structure in the vicinity of 19.8 kHz are detected, suggesting a possible interaction between the NWC signal and radiation from China's power system.

1. Introduction

Power line harmonic radiation (PLHR) refers to a kind of electromagnetic wave phenomena at harmonic frequencies of 50 or 60 Hz that were usually detected in the ionosphere and magnetosphere with frequency range in the ELF and VLF band. Power line emission (PLE) is a special kind of emission with frequencies exactly at 50 or 60 Hz. PLHR and PLE are believed to be related with ground electric power systems since their frequencies have good agreements with corresponding ground power system frequencies. Since 1970s ground observations has been reported from several high-latitude stations [1-3]. Since the launch of DEMETER satellite, lots of PLHR and PLE observations have been reported [4,5]. Other events have also been observed by "Chibis-M" [6].

As a recognized man-made pollutant in near-Earth space, the environmental effect on the ionosphere caused by PLHR and PLE has become an increasing concern [7]. They may interact with particles and other natural or man-made waves, causing wave growths, triggering emissions and electron precipitations, altering the states of the ionosphere [8,9].

It is necessary to conduct statistically research of the ionosphere states due to the influence of radiation from terrestrial power sources. By scanning the observed data of 6.5 operating years of DEMETER satellite, 133 PLHR events with central frequencies from 500 Hz to 4.5 kHz have been detected in the near-Earth space above China [10]. Section 2 firstly introduces the data set and processing method, and then gives two examples showing the characteristics of PLHR and PLE. Based on the 133 events, we investigated the relation between PLHR and PLE in section 3. Section 4 presents 2 events with the harmonic line structure radiation in the vicinity of 19.8 kHz which is exactly

Content from this work may be used under the terms of the Creative Commons Attribution 3.0 licence. Any further distribution of this work must maintain attribution to the author(s) and the title of the work, journal citation and DOI.
Published under licence by IOP Publishing Ltd

the frequency band of the Australian NWC VLF transmitter. Finally, the conclusion is summarized in section 5.

2. Processing method of satellite data set and examples showing PLHR and PLE

2.1. Introduction of satellite data set and processing method

DEMETER was a French seismo-electromagnetic microsatellite with a nearly Sun-synchronous circular orbit operating at 710 km (lower to 650 km at the end of 2005). It operated from July, 2004 to December, 2010. It passed over a specific region with a local time ~10:30 LT during daytime and ~22:30 LT during nighttime. The electric field waveform data were used to identify PLHR events. The Systems Tool Kit (STK) was used to extract the orbit through DEMETER operation years (2004 to 2010) and 5690 half-orbit data files covering China (a rectangle defined by: 12°N to 53°N and 75°E to 135°E) were downloaded for analysis. Some data covered not only China but also adjacent areas. There are about hundreds to at most three thousand of data groups in each half-orbit file and 8192 sampling waveform data per group. The sampling frequency is 40 kHz. The short-time Fourier transform (STFT) was used to analyze the time-frequency power spectral density (PSD) of the electric field strength. A frequency-time spectrogram with a frequency resolution of 4.8828Hz and time resolution of 0.8192s could be obtained.

An automatic PLHR detecting program based on the PSD spectrogram was developed. We detect spectral lines related to PLHR by comparing each line with two adjacent lines, up and down, respectively. If the power density of the k-th line is defined as P_k, the following three types of lines are considered to have PLHR character:

- P_k is 7dB larger than P_{k-1} and P_{k+1}.
- P_k is 6dB larger than P_{k-1} and P_{k+2}, and P_{k+1} was 6dB larger than P_{k+2}.
- P_k is 6dB larger than P_{k-2} and P_{k+1}, and P_{k-1} was 6dB larger than P_{k-2}.

If these lines last more than 4.1 s and the total break time during the detection process was less than 2.46s, they were regarded as “potential” PLHR event and selected for manual inspection. The threshold values for power density, duration and break time could be adjusted according to the specific orbit. Then we used the Welch power spectra estimation method to draw the power density spectra of “potential” PLHR events. The discussed time duration was divided into several sections to avoid strong interference from whistlers, chorus and other VLF emissions in the same frequency band. We combined these sections and analyzed them using a 40,000-point FFT with 75% overlapping and the Hanning window. We obtained the final spectra with a resolution of 1 Hz. Finally, 133 PLHR events above China were detected in total.

2.2. Examples of PLHR and PLE

Figure 1 shows a typical PLHR and PLE event detected around Universal Time 02:35 on Nov. 17, 2010 when the satellite was just above China. Figure 1(a) and 1(b) is the frequency-time spectrogram and power spectrum of the PLHR event. From figure 1(a)(b), we can see the 4 spectral lines locating at about 4150, 4250, 4350 and 4450 Hz with frequency spacing 100 Hz. The dashed line in figure 1(b) is the average power density. Figure 1(c) is the frequency-time spectrogram of the PLE event. The 50 Hz spectral line in figure 1(c) is the PLE event. The intensive vertical lines are whistlers in the ionosphere. Figure 1(d) shows the satellite trajectory (black line) and geophysical duration of the PLHR (red line) and PLE (blue line) events.

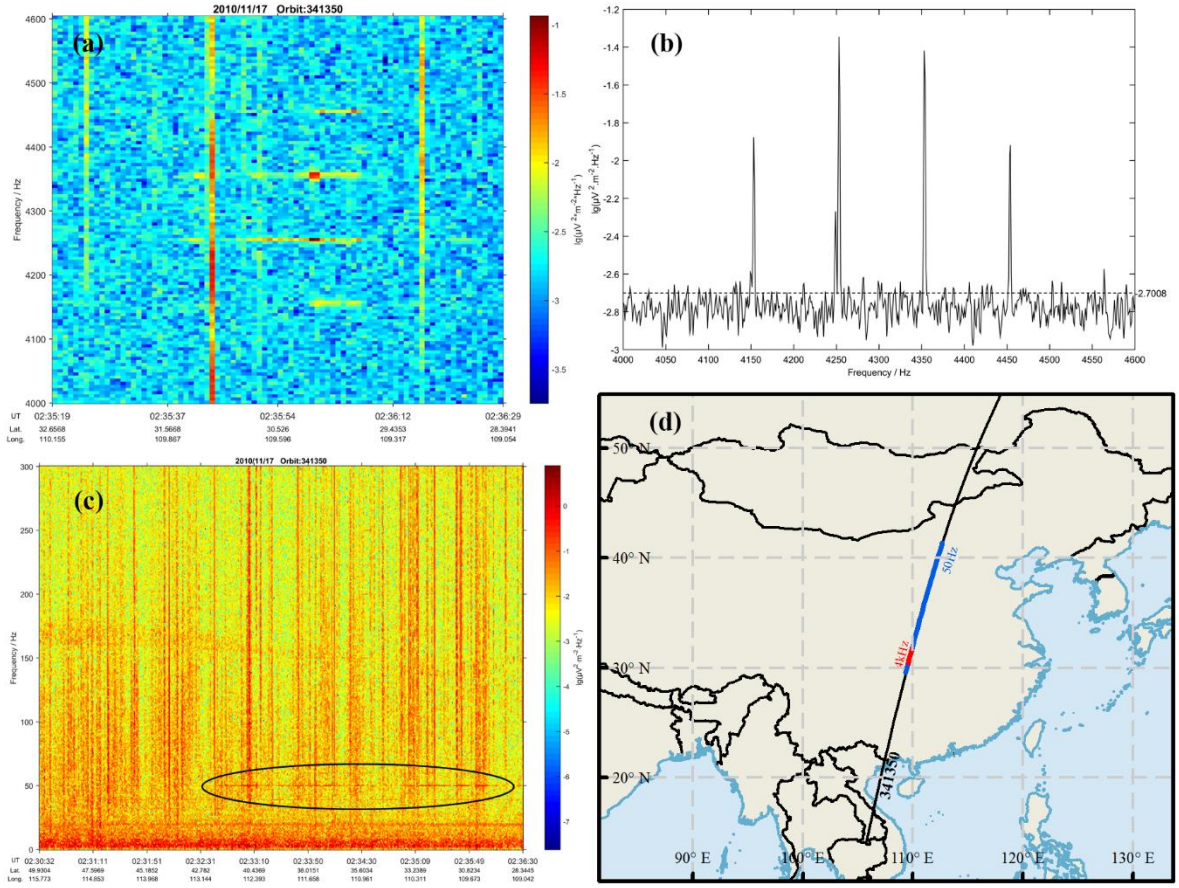


Figure 1. An example of PLHR and PLE event. (a) Spectrogram of the PLHR event with frequencies 4k-4.6kHz. (b) Power spectrum of the PLHR event. (c) Spectrogram of the corresponding PLE event. (d) Satellite trajectory and geolocation of the events.

Figure 2 is an example showing the frequency conversion on the same orbit when the satellite flew over different nations or regions. The orbit was on Dec. 16, 2004 when the satellite was upgoing crossing Philippines and China successively. The 60 Hz spectral line in figure 2(b) corresponds to the blue line in figure 2(a) when the satellite flew over Philippines. The 50 Hz spectral line in figure 2(c) corresponds to red line when the satellite flew over China. The frequencies relate very well to the fundamental frequencies of ground power systems of the two countries: i.e., Philippines adopts 60 Hz power system while China adopts 50 Hz.

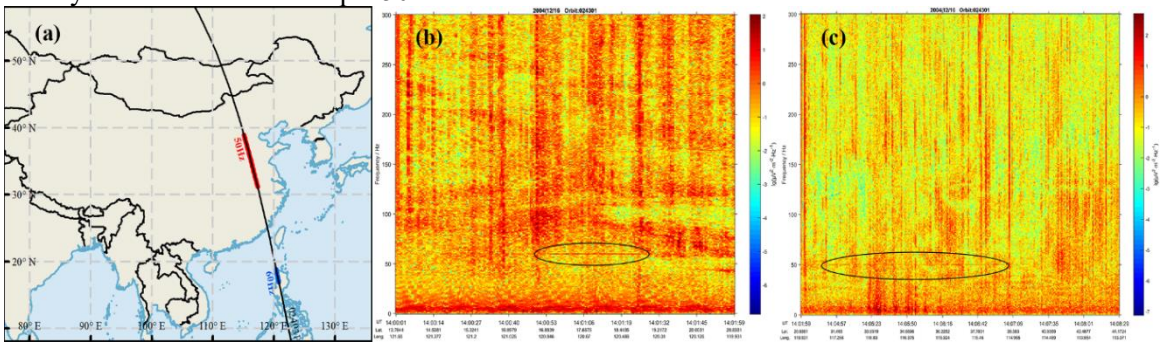


Figure 2. The two PLE events with different frequencies detected on the same orbit when the satellite flew over Philippines and China successively. (a) Satellite trajectory and geolocation of the two PLE events. (b) Spectrogram of the 60 Hz PLE event when the satellite flew over Philippines. (c) Spectrogram of the 50 Hz PLE event when the satellite flew over China.

3. Relation of PLHR and PLE events

Among the 133 PLHR events, 129 events have PLE events at the power system fundamental frequency (50 Hz in China). The duration of every PLE event covers that of the corresponding PLHR event totally. Figure 3 is an example showing the relation of PLHR and PLE. There are 3 PLE events with 50 Hz. There are 2 PLHR events with frequencies at the range 2-3.5 kHz and 4-4.5 kHz, and they correspond to the second and third PLE respectively.

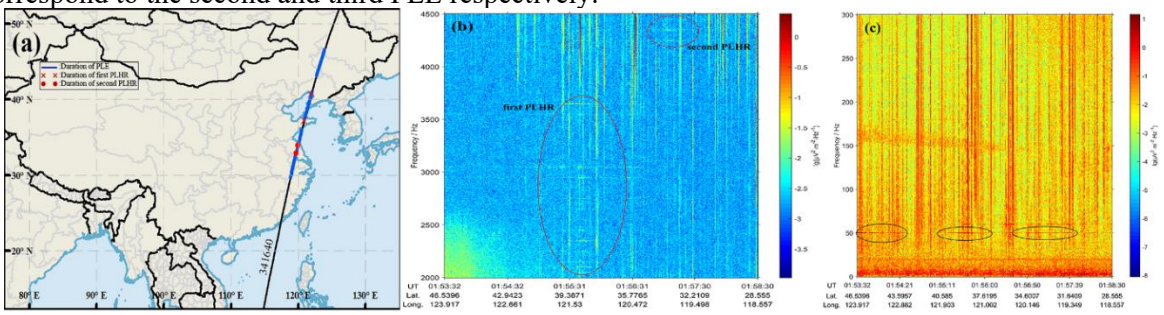


Figure 3. An example showing the relation of PLHR and PLE. (a) Satellite trajectory, 3 PLEs and 2 PLHRs; (b) Spectrogram of the 2 PLHR events; (c) Spectrogram of the 2 PLE events.

PLEs are more detectable than PLHRs observed by DEMETER satellite. As seen from figure 1(c), weak 60 Hz lines can often be detected in east coast of China. They suggest Earth-ionosphere waveguide propagation from Korea or the west Japan which adopt 60 Hz power system. After penetration into the ionosphere, as the same with PLHR, PLE propagates along the geomagnetic field line in the whistler mode in the ionosphere. Figure 4 shows the 3 components of electric field power density spectrogram of figure 1(c) in Local GEOMagnetic coordinate. The origin is at the center of the satellite. *Z-direction* is parallel to the geomagnetic field line.

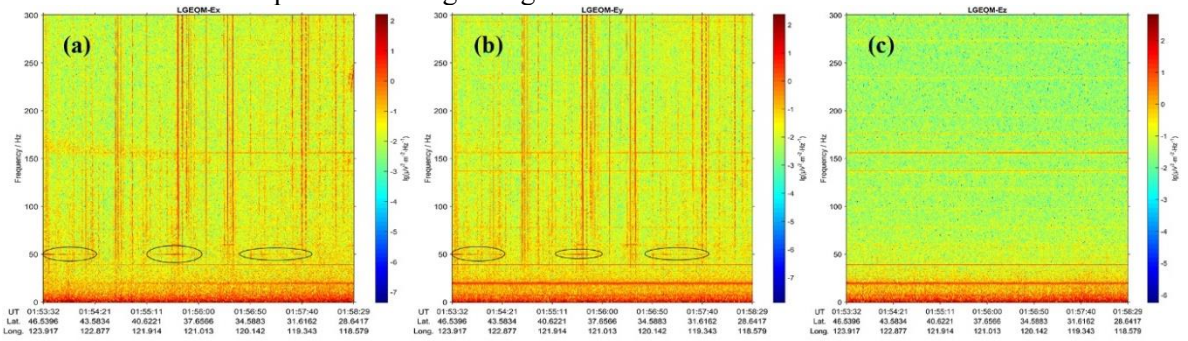


Figure 4. Three components of the electric field in local geomagnetic coordinate. PLEs exist only in perpendicular directions (*X*- and *Y-direction*) of the local geomagnetic field, propagate along the geomagnetic field line in whistler mode.

4. Harmonic line structure radiation related to the NWC transmitter

In two events that occurred in the conjugate region of Australian NWC VLF transmitter, radiations with harmonic line structure in the vicinity of 19.8 kHz are detected. There are several obvious lines distributed from about 19.7 kHz to 19.9 kHz, which are in accordance with the frequency range of NWC transmitted signals. The frequency spacings of these lines are exactly 50 or 100 Hz and the bandwidth of each line is about 10 Hz. The NWC signal was modulated into this harmonic line structure radiation, suggesting possible interaction between NWC signals and radiations from China's power system.

Figure 5 shows the harmonic line structure radiation and the spectra of 3 frequency bands, PLE band, PLHR band (1-1.5 kHz) and the NWC frequency band. The time in the NWC frequency band is divided into 3 sections as shown in the left panel, and their spectra are presented in different colors in the right panel.

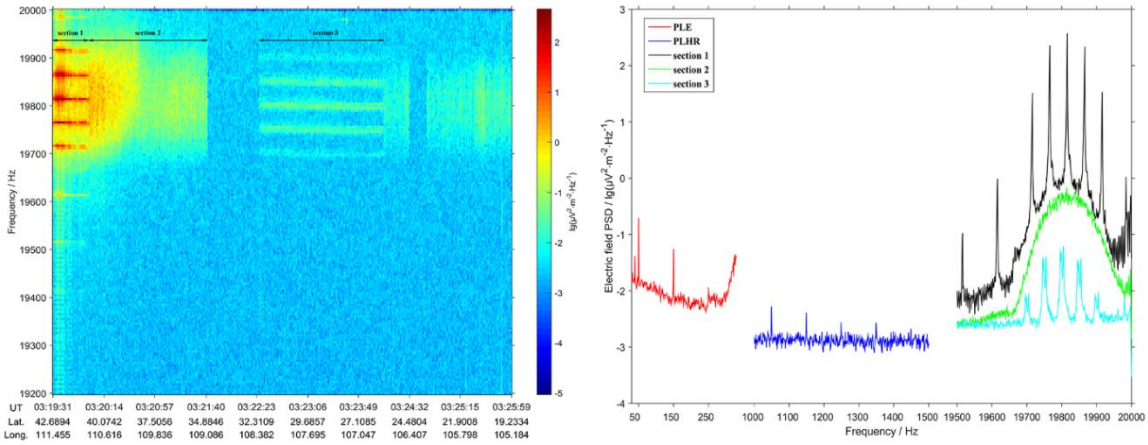


Figure 5. Harmonic line structure radiation and the spectra in 3 frequency bands.

5. Conclusions

Based on DEMETER satellite observed data, this paper detected the PLHR and PLE events in the ionosphere above China and analysed the characteristics and relation of the two kinds of radiations. Finally, the harmonic line structure radiation related to the NWC VLF transmitter was investigated, suggesting possible modulation of NWC signals by radiations from China's power system. The conclusions are as follows.

- The fundamental frequency related very well to the frequency of corresponding ground power system.
- Nearly all the PLHR events have corresponding PLEs at the fundamental frequency of local power system. PLEs have no electric field component in the direction of geomagnetic field, propagate along the field line in whistler mode.
- The harmonic line structure radiation in the conjugate region of Australian NWC VLF transmitter suggest a probable interaction between the NWC signal and radiation from China's power system which calls for a further investigation.

References

[1] Helliwell R A, Katsufrakis J P, Bell TF and Raghuram R 1975 *J. Geophys. Res.* **80** 4249–58
[2] Matthews J P and Yearby K 1981 *Planet. Space Sci.* **29** 97-106
[3] Manninen J 2005 Some aspects of ELF-VLF emissions in geophysical research PhD thesis (Oulu: Univ. of Oulu, Finland) chapter 4 pp 59-63
[4] Němec F, Santolík O, Parrot M, Berthelier J J 2006 *J. Geophys. Res.* **111** A04308
[5] Němec F, Parrot M, Santolík O 2015 *J. Geophys. Res. Sp. Phys.* **120** 8954-67
[6] Dudkin F, Korepanov V, Dudkin D, Pilipenko V, Pronenko V and Klimov S 2015 *Geophys. Res. Lett.* **42** 5686-93
[7] Parrot M and Zaslavski Y 1996 *Surv. Geophys.* **17** 67–100
[8] Němec F, Parrot M and Santolík O 2010 *J. Geophys. Res. Sp. Phys.* **115** A11301
[9] Parrot M, Němec F and Santolík O 2014 *J.Geophys. Res. Sp. Phys.* **119** 5744-54
[10] Wu J, Zhang C, Zeng L and Ma Q S 2017 *J.Geophys. Res. Sp. Phys.* **122** 3448-58